

BPC 01093

TOTAL INTERNAL REFLECTION FLUORESCENCE

MEASUREMENT OF SPATIAL AND ORIENTATIONAL DISTRIBUTIONS OF FLUOROPHORES NEAR PLANAR DIELECTRIC INTERFACES

Nancy L. THOMPSON ^a and Thomas P. BURGHARDT ^b

^a Department of Chemistry, University of North Carolina at Chapel Hill, Chapel Hill, NC 27514, and ^b 841 Health Sciences West, Cardiovascular Research Institute, University of California at San Francisco, San Francisco, CA 94143, U.S.A.

Received 25th June 1986

Accepted 4th August 1986

Key words: Evanescent wave; Ordered biological assembly; Solid/liquid interface; Order parameter; Fluorescence microscopy

The fluorescence collected from a fluorophore which is near a planar interface and is excited by a laser beam that is totally internally reflected at the interface depends on the direction of the absorption and emission transition dipole moments of the fluorophore with respect to the interface, on the distance from the fluorophore to the interface, on the angle of incidence and polarization direction of the exciting beam, and on properties of the collection optics. Expressions are derived for the excitation and subsequent emission and collection of fluorescence from a population of fluorophores near a planar interface. Presented is a general model-independent method of obtaining characteristic parameters of the spatial and orientational distribution of the population of fluorophores, from a measure of the fluorescence collected as a function of the polarization and the incidence angle of the totally internally reflected laser beam. The method is illustrated with several simulation calculations.

1. Introduction

Total internal reflection fluorescence (TIRF) is a technique for selectively exciting fluorescent molecules near a planar dielectric interface [1]. When combined with fluorescence microscopy [2], this technique is useful for measuring the association/dissociation rates and surface diffusion coefficient of fluorescent-labelled molecules at surfaces [3–6], measuring orientational distributions of fluorescent probes at or near surfaces [7,8], observing fluorescent molecules in cell-surface contact regions [9–14], detecting conformation changes of proteins at surfaces [15,16], and measuring the concentration profiles of fluorescent polymers near surfaces [17,18]. In general, the fluorescence collected from a fluorescent molecule that is excited by a totally internally reflected light beam depends on the direction of the absorption and

emission transition dipole moments of the fluorophore with respect to the interface, on the distance from the molecule to the interface, on the angle of incidence of the exciting beam, on the polarization of the exciting light, and on properties of the collection optics.

In this paper, we derive general expressions for the excitation and subsequent emission and collection of fluorescence from molecules in a TIRF experiment. Presented is a general, model-independent method of obtaining characteristic parameters of the spatial and orientational distribution of a population of molecules near a dielectric interface, from a measure of the fluorescence collected as a function of the polarization and the incidence angle of the totally internally reflected light beam. The method is illustrated with several simulation calculations.

2. Theoretical basis

A planar interface of glass (refractive index $n_g = 1.5$) and water (refractive index $n_w = 1.33$) is defined as the xy plane, with positive z in the glass region. A laser beam of vacuum wavelength λ_0 is incident on the interface in the xz plane, with incidence angle α and polarization angle β (fig. 1). The angle α is greater than the critical angle $\alpha_c = \sin^{-1}n$, where $n = n_w/n_g$, so that the beam totally internally reflects at the interface. This produces an electromagnetic field in the water region, called the 'evanescent field', that excites fluorescent molecules at or near the interface.

The following assumptions are made: (1) the fluorescence lifetime is much shorter than the rotational correlation time and than the characteristic times of diffusion through the observation area and the depth of the evanescent field; and (2) the angle between the absorption and emission transition dipole moments is zero. Then, the fluorescence intensity $F(\alpha, \beta)$ collected from a population of molecules with spatial and orientational distribution $N(\hat{a}, z)$, where \hat{a} is a unit vector pointing in the direction of the transition dipole moment and z is the distance from the interface, and for an exciting laser beam of polarization β

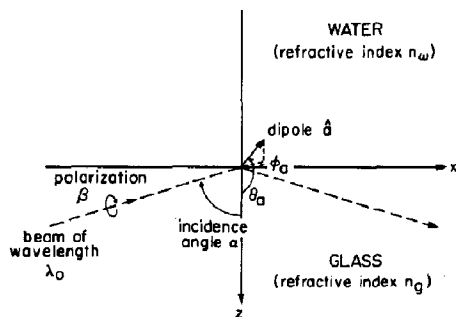


Fig. 1. Excitation of fluorescent molecules with evanescent illumination. A light beam of vacuum wavelength λ_0 is incident on a planar interface of glass (refractive index n_g) and water (refractive index $n_w < n_g$) at an angle α greater than the critical angle for total internal reflection. The interface is defined as the xy plane and the light beam is incident in the xz plane. The light beam is linearly polarized at an angle β from its incidence plane. A transition dipole with a direction denoted by \hat{a} is excited by the evanescent field and emits fluorescence.

and incidence angle α is

$$F(\alpha, \beta) = \int_0^\infty \int_{\Omega_0} \int_{\Omega_{\text{obs}}} N(\hat{a}, z) A(\hat{a}, z, \alpha, \beta) \times f(\hat{a}, z, \hat{p}) d\Omega_p d\Omega_a dz. \quad (1)$$

$A(\hat{a}, z, \alpha, \beta)$ is the absorptivity of a molecule which is a distance z from the interface and has its transition dipole moment along unit vector $\hat{a}(\theta_a, \phi_a)$, and $f(\hat{a}, z, \hat{p})$ is the fluorescence intensity emitted into the direction of unit vector $\hat{p}(\theta_p, \phi_p)$ by the molecule. The domain of integration over \hat{a} , Ω_0 , is over all angular space; the domain of integration over \hat{p} , Ω_{obs} , is over the angles observed by a particular experimental apparatus.

The absorptivity A is given by [7,19]

$$A(\hat{a}, z, \alpha, \beta) = \exp(-z/d) \left[I_x \cos^2 \beta a_x^2 + I_y \sin^2 \beta a_y^2 + I_z \cos^2 \beta a_z^2 + 2 \cos \beta \sin \beta (I_{xy} a_x a_y + I_{yz} a_y a_z) \right], \quad (2)$$

where d , the characteristic depth of the evanescent field, is equal to [2]

$$d(\alpha) = \lambda_0 / \left[4\pi n_g (\sin^2 \alpha - n^2)^{1/2} \right], \quad (3)$$

and the factors I are known functions of n and α and have been given earlier [7].

The angular profile of the emitted fluorescence $f(\hat{a}, z, \hat{p})$ is given by

$$f(\hat{a}, z, \hat{p}) = R_r(\hat{a}, z, \hat{p}) Q(\hat{a}, z) / P(\hat{a}, z). \quad (4)$$

$R_r(\hat{a}, z, \hat{p})$ is the rate of radiative (fluorescence) emission of an excited fluorophore, and has been shown to equal [8]

$$R_r(\hat{a}, z, \hat{p}) = \left[f_x a_x^2 + f_y a_y^2 + f_z a_z^2 + f_{xy} a_x a_y + f_{xz} a_x a_z + f_{yz} a_y a_z \right], \quad (5)$$

where the factors f depend on \hat{p} and z , and not on \hat{a} , and are given below. Function $Q(\hat{a}, z)$ is the quantum efficiency and is given by

$$Q(\hat{a}, z) = P(\hat{a}, z) / (P(\hat{a}, z) + R_{nr}), \quad (6)$$

where $P(\hat{\mathbf{a}}, z)$ is the radiative rate summed over all observation angles, or

$$P(\hat{\mathbf{a}}, z) = \int_{\Omega_0} R_r(\hat{\mathbf{a}}, z, \hat{\mathbf{p}}) d\Omega_p, \quad (7)$$

and R_{nr} is the rate of radiationless decay, which is assumed to be independent of $\hat{\mathbf{a}}$, $\hat{\mathbf{p}}$ and z . The function $P(\hat{\mathbf{a}}, z)$ is explicitly present in eq. 4 as a normalization factor because the power emitted from equally excited molecules must be independent of $\hat{\mathbf{a}}$ and z when $Q(\hat{\mathbf{a}}, z) = 1$ [20]. Using eq. 6 evaluated at $z = \infty$, and defining $Q_0 = Q(\hat{\mathbf{a}}, \infty)$ as the (known) quantum efficiency in homogeneous space, we can determine R_{nr} in terms of Q_0 and $P(\hat{\mathbf{a}}, \infty)$. Using the resultant expression for R_{nr} in eq. 6 evaluated for all z , and using this expression in eq. 4, we find that

$$f(\hat{\mathbf{a}}, z, \hat{\mathbf{p}}) = Q_0 R_r(\hat{\mathbf{a}}, z, \hat{\mathbf{p}}) / [Q_0 P(\hat{\mathbf{a}}, z) + (1 - Q_0) P(\hat{\mathbf{a}}, \infty)]. \quad (8)$$

Different expressions for the factors $f_{x,y,z}$ exist in three different spatial regions. In the water ($\pi/2 \leq \theta_p \leq \pi$),

$$\begin{aligned} f_{x,y} &= (R_{\parallel}^2 - hR_{\parallel} + 1) \cos^2 \theta_p (\cos^2 \phi_p, \sin^2 \phi_p) \\ &\quad + (R_{\perp}^2 + hR_{\perp} + 1) (\sin^2 \phi_p, \cos^2 \phi_p) \\ f_z &= (R_{\parallel}^2 + hR_{\parallel} + 1) \sin^2 \theta_p \end{aligned} \quad (9)$$

where

$$R_{\parallel,\perp} = \frac{(1, n) \cos \theta_p + (n, 1) (1 - n^2 \sin^2 \theta_p)^{1/2}}{(1, n) \cos \theta_p - (n, 1) (1 - n^2 \sin^2 \theta_p)^{1/2}} \quad (10)$$

$$h = 2 \cos \{ (2kn_w \cos \theta_p) z \}$$

$$k = 2\pi/\lambda_0.$$

In the glass below the critical angle ($0 < \theta_p < \alpha_c$), the factors $f_{x,y,z}$ are given by

$$\begin{aligned} f_{x,y} &= T_{\parallel}^< (|n^2 - \sin^2 \theta_p|/n^2) (\cos^2 \phi_p, \sin^2 \phi_p) \\ &\quad + T_{\perp}^< (\sin^2 \phi_p, \cos^2 \phi_p) \\ f_z &= T_{\parallel}^< \sin^2 \theta_p / n^2 \end{aligned} \quad (11)$$

where

$$T_{\parallel,\perp}^< = 4(n^2, 1) \cos^2 \theta_p / \left[(n^2 - \sin^2 \theta_p)^{1/2} + (n^2, 1) \cos \theta_p \right]^2. \quad (12)$$

In the glass above the critical angle ($\alpha_c < \theta_p < \pi/2$), the factors $f_{x,y,z}$ are given by eq. 11 where $T_{\parallel,\perp}^<$ are replaced by $T_{\parallel,\perp}^>$,

$$\begin{aligned} T_{\parallel}^> &= 4 \exp[-z/d(\theta_p)] n^2 \cos^2 \theta_p / \\ &\quad \left[(1 - n^2) - (1 - n^4) \cos^2 \theta_p \right] \\ T_{\perp}^> &= 4 \exp[-z/d(\theta_p)] \cos^2 \theta_p / (1 - n^2), \end{aligned} \quad (13)$$

and d is given in eq. 3. In all regions,

$$\begin{aligned} f_{xy} &\sim \sin \phi_p \cos \phi_p \\ f_{xz,yz} &\sim (\cos \phi_p, \sin \phi_p). \end{aligned} \quad (14)$$

We define a new function

$$S(\hat{\mathbf{a}}, z, \alpha, \beta) = A(\hat{\mathbf{a}}, z, \alpha, \beta) \times \int_{\Omega_{\text{obs}}} f(\hat{\mathbf{a}}, z, \hat{\mathbf{p}}) d\Omega_p, \quad (15)$$

so that, from eq. 1,

$$F(\alpha, \beta) = \int_0^\infty \int_{\Omega_0} N(\hat{\mathbf{a}}, z) S(\hat{\mathbf{a}}, z, \alpha, \beta) d\Omega_a dz. \quad (16)$$

Functions $S(\hat{\mathbf{a}}, z, \alpha, \beta)$ and $N(\hat{\mathbf{a}}, z)$ are expanded in the spherical harmonics $Y_{ij}(\hat{\mathbf{a}})$ and in the following functions of z :

$$W_m(kz) = \exp(-kz/2) L_m(kz), \quad (17)$$

where L_m are Laguerre polynomials and k is the vacuum wave number for the excitation light given in eqs. 10. In the expansion, we write

$$N(\hat{\mathbf{a}}, z) = \sum_{ijm} N_{ijm} W_m(z) Y_{ij}(\hat{\mathbf{a}}) \quad (18)$$

$$\begin{aligned} S(\hat{\mathbf{a}}, z, \alpha, \beta) &= \sum_{ijm} s_{ijm}(\alpha, \beta) W_m(z) Y_{ij}(\hat{\mathbf{a}}) \\ &= \sum_{ijm} s_{ijm}^*(\alpha, \beta) W_m(z) Y_{ij}^*(\hat{\mathbf{a}}), \end{aligned} \quad (19)$$

where the final equality results from the fact that $S(\hat{a}, z, \alpha, \beta)$ is real. The orthogonalities of the functions Y_{ij} and W_m imply that

$$\int_{\Omega_0} Y_{ij}^*(\hat{a}) Y_{i'j'}(\hat{a}) d\Omega_a = \delta_{i,i'} \delta_{j,j'} \quad (20)$$

$$\int_0^\infty W_m(z) W_{m'}(z) dz = \delta_{m,m'}, \quad (21)$$

where $\delta_{i,j}$ is the Kronecker delta. Substituting eqs. 18 and 19 into eq. 16 and using eqs. 20 and 21, we find that

$$F(\alpha, \beta) = \sum_{ijm} N_{ijm} s_{ijm}^*(\alpha, \beta). \quad (22)$$

Eqs. 18–21 also imply that

$$N_{ijm} = \int_0^\infty \int_{\Omega_0} N(\hat{a}, z) W_m(z) Y_{ij}^*(\hat{a}) d\Omega_a dz \quad (23)$$

$$s_{ijm}^*(\alpha, \beta) = \int_0^\infty \int_{\Omega_0} S(\hat{a}, z, \alpha, \beta) W_m(z) \times Y_{ij}(\hat{a}) d\Omega_a dz. \quad (24)$$

Moments N_{ijm} describe the orientational and spatial distribution of fluorophores $N(\hat{a}, z)$, and are what we wish to obtain from measurement of $F(\alpha, \beta)$. Using these moments, the function $N(\hat{a}, z)$ can be reconstructed with eq. 18. As shown in eq. 22, the measured function $F(\alpha, \beta)$ is built up from a linear combination of the functions $s_{ijm}^*(\alpha, \beta)$, with coefficients N_{ijm} . These functions $s_{ijm}^*(\alpha, \beta)$ can be numerically calculated using eq. 24 and the known numerically integrated form of $S(\hat{a}, z, \alpha, \beta)$ given in eq. 15, obtained from eqs. 2–14. The functions $s_{ijm}^*(\alpha, \beta)$ can be thought of as a set of basis functions that spans the space occupied by all possible measured functions $F(\alpha, \beta)$. Our task is to measure the amount of each basis function, i.e., the value of N_{ijm} , contained in the measured function $F(\alpha, \beta)$. As shown in an earlier paper [19], the values of N_{ijm} are given by

$$N_{ijm} = \sum_{i'j'm'} \int_0^\infty \int_{\alpha_0}^{\pi/2} c_{ijm;i'j'm'} s_{i'j'm'}^*(\alpha, \beta) \times F(\alpha, \beta) d\alpha d\beta, \quad (25)$$

where $c_{ijm;i'j'm'}$ is the $(ijm, i'j'm')$ -th element of

the inverse of the matrix with elements

$$\int_0^\pi \int_0^{\pi/2} s_{ijm}^*(\alpha, \beta) s_{i'j'm'}^*(\alpha, \beta) d\alpha d\beta. \quad (26)$$

The protocol for data analysis is as follows. Using eqs. 2–14, $S(\hat{a}, z, \alpha, \beta)$ is calculated; using eq. 24, the $s_{ijm}^*(\alpha, \beta)$ are calculated; the matrix in eq. 26 is calculated and inverted to give the values of $c_{ijm;i'j'm'}$. The basis function set $s_{ijm}^*(\alpha, \beta)$ and the matrix $c_{ijm;i'j'm'}$ are stored permanently and used in any experiment, simulated or real. For a particular $F(\alpha, \beta)$, the coefficients N_{ijm} are then calculated using eq. 25. $N(\hat{a}, z)$ can be reconstructed using eq. 18.

3. Simulation calculations

In this section, we have tested the method outlined above using numerical simulations. We have made several investigations into the forms of $N(\hat{a}, z)$ that might be readily measured with the described technique. To do this, a form for $N(\hat{a}, z)$ that might exist in an experimental sample is postulated, and denoted by N_{actual} . Several of the lowest order values of N_{ijm} for this distribution are calculated using eq. 23 and are denoted by $(N_{ijm})_{\text{actual}}$. Using $N(\hat{a}, z) = N_{\text{actual}}$ in eq. 1, along with eqs. 2–14, we calculate $F(\alpha, \beta)$ as it would be observed in the experiment, and denote this function by $F_{\text{obs}}(\alpha, \beta)$. Next, we calculate the values of N_{ijm} from eq. 25, using the permanently stored values of $s_{ijm}^*(\alpha, \beta)$ and $c_{ijm;i'j'm'}$, and with $F(\alpha, \beta) = F_{\text{obs}}(\alpha, \beta)$. The calculated values of N_{ijm} , denoted by $(N_{ijm})_{\text{obs}}$, are compared to the values of $(N_{ijm})_{\text{actual}}$.

We have assumed that all of the fluorescence emitted into the water half-space $z < 0$ is collected with a high-aperture microscope objective (e.g., ref. 7), so that Ω_{obs} denotes $0 \leq \phi_p \leq 2\pi$ and $\pi/2 \leq \theta_p \leq \pi$. In addition, we have assumed that the quantum efficiency in homogeneous space, Q_0 , is 1. In general, however, the methods presented in this paper are applicable to any optical collection geometry and to fluorophores with any quantum efficiency Q_0 .

We have also confined the simulation calculations to distributions $N(\hat{a}, z)$ that depend only on

z and not \hat{a} . A similar but less comprehensive method of obtaining the expansion coefficients of the orientational distribution of a population of fluorophores that is on the interface at $z=0$ has previously been developed and applied to fluorescent molecules in planar phospholipid monolayers deposited on hydrophobic surfaces [7]. In general, the methods presented in this paper are applicable to a distribution $N(\hat{a}, z)$ that depends only on \hat{a} , only on z , or on both.

3.1. Randomly oriented in solution

In this case, the fluorophores are assumed to be randomly distributed in angle and space, and we use the normalization $N_{\text{actual}} = 1/8\pi$. We find that the first six calculated expansion coefficients, $(N_{00m})_{\text{obs}}$, $m=0, 5$, agree with the values of $(N_{00m})_{\text{actual}}$ to within at least 2.0%.

3.2. Randomly oriented in a plane

Phospholipid bilayers deposited on planar substrates have been employed in a number of recent biophysical investigations [22–25]. However, it is not yet known if a layer of water exists between the phospholipid bilayer and the glass, and, if so, what the thickness of this layer is for different deposition procedures. The existence of such a layer is important for the reconstitution of purified transmembrane proteins in supported planar bilayers. The proposed technique may be able to measure these distances. Thus, we have investigated a case in which the fluorophores are assumed to be randomly oriented in a plane a distance b from the interface. We have used the normalization

$$N_{\text{actual}} = (1/4\pi)\delta(kz - kb). \quad (27)$$

We would like to know the range of distances b that can be measured with the described technique of data analysis.

The values of the first five expansion coefficients $(N_{00m})_{\text{obs}}$, $m=0, 4$, are plotted in fig. 2a for values of b ranging from 0 to $5/k$ (~ 4000 Å). For low values of b , the values of $(N_{00m})_{\text{obs}}$ agree with the values of $(N_{00m})_{\text{actual}}$ to within an average of $\leq 2\%$. For higher values of b , a few of the

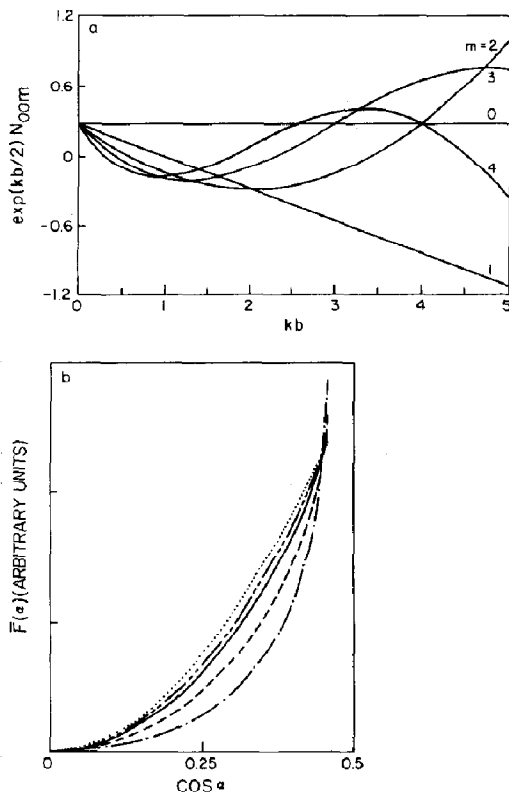


Fig. 2. Delta-function distribution. (a) The product of $\exp(kb/2)$ and the expansion coefficients $(N_{00m})_{\text{obs}}$ for $m=0, 4$, are shown for the distribution given in eq. 27, for different distances b from the interface of the plane that contains the fluorophores. Assumed is that the vacuum wavelength of the exciting light is 5000 Å. (b) The fluorescence intensity $F(\alpha)$ defined in eq. 28 that would be observed for different distances $b=0$ (.....), $b=0.1/k$ (----), $b=0.2/k$ (—), $b=0.5/k$ (----) and $b=1/k$ (-.-.-).

values of $(N_{00m})_{\text{obs}}$ deviate from the values of $(N_{00m})_{\text{actual}}$ by as much as 20%, but only for low values (≈ 0) of N_{00m} . As shown, for small values of b , $\exp(kb/2)N_{00m}$ are linearly dependent on b , and distinction between different b values depends primarily on the accuracy with which $F(\alpha, \beta)$ can be measured. Ausserré et al. [18] achieved 0.02 degree resolution. In fig. 2b are shown the functions

$$\bar{F}(\alpha) = (2/\pi) \int_0^{2\pi} F(\alpha, \beta) d\beta \quad (28)$$

that would be measured for different b values. Assuming an experimental precision of a few percent, one can thus distinguish between $b = 0$, $b = 0.1/k \approx 80$ Å and $b = 0.2/k \approx 160$ Å.

3.3. Other distributions

Ausserré et al. [18] have used TIRF to study the concentration profile of fluorescent-labelled polymers in solution near a planar surface. In this case, the fluorophores are assumed to be randomly oriented with a concentration profile N_{actual} proportional to $\tanh^2(z/b)$, where b is a length characteristic of the depletion layer of polymers near the interface. We have tested this distribution with the described method and with $b = 800$ Å, and have found that the values of $(N_{00m})_{\text{obs}}$ agree with the values of $(N_{00m})_{\text{actual}}$, for $m = 0, 5$, to within 6%.

4. Discussion

We have presented a general, model-independent procedure for measuring the expansion coefficients (or order parameters) of the spatial and orientational distribution of a population of fluorescent or fluorescent-labelled molecules near a planar dielectric interface. In the procedure, the fluorescence that is excited by a totally internally reflected laser beam is collected as a function of the polarization of the incident beam and as a function of its incidence angle. In simulation calculations, it has been demonstrated that the procedure can determine the values of the expansion coefficients with high accuracy, and that the main limitation in experimental application will depend on the accuracy with which the fluorescence intensity can be measured.

In the simulation calculations, it was assumed that all of the fluorescence emitted into the half-space $z < 0$ was collected and that the quantum efficiency in homogeneous space Q_0 was 1. However, the methods presented in this paper are in general applicable to any collection geometry and to fluorophores with any quantum efficiency Q_0 .

We have also assumed that the fluorescence lifetime is much shorter than the characteristic

time for diffusion through the observation area and through the depth of the evanescent field. For a high diffusion coefficient (10^{-6} cm²/s), the average time for diffusion through a small observation area ($1 \mu\text{m}^2$) is 2.5 ms and the average time for diffusion through the evanescent field is 0.1 ms [26].

Implicit in the described procedure is the assumption of a planar interface between media with different refractive indices. Although dilute solutions or thin molecular layers should not alter the reflective and refractive behavior of light near the interface, large perturbations due to the sample refractive index away from the refractive index of water could alter this behavior. The described technique would not be applicable in these situations.

For the model distributions that we have tested, the described procedure can determine expansion coefficients in the spatial distribution of randomly oriented fluorophores, N_{00m} , through $m \leq 5$.

Previous experiments that have aimed at measuring the expansion coefficients of the angular distribution, N_{ij0} , have been more limited than the technique described in this paper. Because of inherent limitations in a standard fluorescence polarization experiment, the highest order expansion coefficient that can be measured is $i = 4$ [27]. With the technique described in this paper, the limitation is removed and one can in theory measure the infinite set of expansion coefficients with $i > 4$. This means that more expansion coefficients can be measured simply by placing a sample on a glass slide. However, we have found in simulation calculations that for $i > 8$, the basis functions begin to overlap, the matrix in eq. 26 becomes singular, and the determination of the corresponding order parameters becomes inaccurate. Thus, in practice, we have extended the limit to $i < 8$.

It is possible to reconstruct the function $N(\hat{a}, z)$ entirely independent of an assumed model, using the measured values of N_{ijm} and eq. 18. In practice, however, the accuracy of the reconstructed function will be limited by how many terms are included in the sum and by how fast the sum converges.

Measurement of the angular distribution function of ordered fluorophores has been the objec-

tive of a number of previous experiments employing fluorescence polarization [7,28,29]. In the past, analysis of fluorescence polarization was model-dependent in that data were fitted to a plausible guess for the functional form of the orientation distribution. Here, as in related papers [7,21,27,30], an approach to this problem in which a model is not required has been presented. The model-independent approach is a good starting point for data analysis before a model is chosen since the expansion coefficients can be related to the free parameters of any model. By this feature the validity of many models can be easily tested. Most importantly, this method removes the bias accompanying a chosen model and allows experimental results to be reported in an unambiguous manner.

Acknowledgements

We thank Daniel Axelrod, Edward Hellen and Robert Fulbright of the University of Michigan for helpful discussions concerning fluorescence emission next to interfaces. This work was supported by National Institutes of Health grant GM37145 (N.T.) and by National Science Foundation Presidential Young Investigator Award DCB 8552986 (N.T.).

References

- 1 N.J. Harrick, *Internal reflection spectroscopy* (Wiley Interscience, New York, 1967).
- 2 D. Axelrod, N.L. Thompson and T.P. Burghardt, *Annu. Rev. Biophys. Bioeng.* 13 (1984) 247.
- 3 N.L. Thompson, T.P. Burghardt and D. Axelrod, *Biophys. J.* 33 (1981) 435.
- 4 T.P. Burghardt and D. Axelrod, *Biophys. J.* 33 (1981) 455.
- 5 N.L. Thompson, *Biophys. J.* 38 (1982) 327.
- 6 N.L. Thompson and D. Axelrod, *Biophys. J.* 43 (1983) 103.
- 7 N.L. Thompson, H.M. McConnell and T.P. Burghardt, *Biophys. J.* 46 (1984) 739.
- 8 T.P. Burghardt and N.L. Thompson, *Biophys. J.* 46 (1984) 729.
- 9 D. Axelrod, *J. Cell Biol.* 89 (1981) 141.
- 10 R.M. Weis, K. Balakrishnan, B.A. Smith and H.M. McConnell, *J. Biol. Chem.* 257 (1982) 6440.
- 11 D. Gingell, I. Todd and J. Bailey, *J. Cell Biol.* 100 (1985) 1334.
- 12 F. Lanni, A.S. Waggoner and D.L. Taylor, *J. Cell Biol.* 100 (1985) 1091.
- 13 T.H. Watts, H.E. Gaub and H.M. McConnell, *Nature* 320 (1986) 179.
- 14 M. Nakache, H.E. Gaub, A.B. Schreiber and H.M. McConnell, *Proc. Natl. Acad. Sci. U.S.A.* 83 (1986) 2874.
- 15 T.P. Burghardt and D. Axelrod, *Biochemistry* 22 (1983) 979.
- 16 G.K. Iwamoto, L.C. Winterton, R.S. Stoker, A. Van Wagenan, J.D. Andrade and D.F. Mosher, *J. Colloid Interface Sci.* 106 (1985) 459.
- 17 C. Allain, D. Ausserré and F. Rondelez, *Phys. Rev. Lett.* 49 (1982) 1694.
- 18 D. Ausserré, H. Hervet and F. Rondelez, *Phys. Rev. Lett.* 54 (1985) 1948.
- 19 T.P. Burghardt and N.L. Thompson, *Opt. Eng.* 23 (1984) 62.
- 20 E.H. Hellen, R.M. Fulbright and D. Axelrod, in: *Spectroscopic membrane probes*, ed. L. Loew (CRC Press, 1986), in the press.
- 21 T.P. Burghardt and N.L. Thompson, *Biophys. J.* 48 (1985) 401.
- 22 L.K. Tamm and H.M. McConnell, *Biophys. J.* 47 (1985) 105.
- 23 S. Subramaniam, N.L. Thompson, L.K. Tamm and H.M. McConnell, *Biophys. J.* 47 (1985) 367a.
- 24 A.A. Brian and H.M. McConnell, *Proc. Natl. Acad. Sci. U.S.A.* 81 (1984) 6159.
- 25 T.H. Watts, A.A. Brian, J.W. Kappler, P. Marrack and H.M. McConnell, *Proc. Natl. Acad. Sci. U.S.A.* 81 (1984) 7564.
- 26 N.L. Thompson, Ph. D. Dissertation, University of Michigan, Ann Arbor, MI (1982).
- 27 T.P. Burghardt, *Biopolymers* 23 (1984) 2383.
- 28 M. Wilson and R. Mendelson, *J. Muscle Res. Cell Motil.* 4 (1983) 671.
- 29 J. Borejdo, O. Assulin, T. Ando and S. Putnam, *J. Mol. Biol.* 158 (1982) 391.
- 30 T.P. Burghardt, T. Ando and J. Borejdo, *Proc. Natl. Acad. Sci. U.S.A.* 80 (1983) 7515.